

## Fluorescence Yields of the $L_{II}$ and $L_{III}$ Shells in Heavy Elements\*

R. C. JOPSON, J. M. KHAN, HANS MARK, C. D. SWIFT, AND M. A. WILLIAMSON  
*Lawrence Radiation Laboratory, University of California, Livermore, California*

(Received 16 August 1963)

A method has been developed to measure the fluorescence yields of the  $L_{III}$  subshells in many heavy elements. This method is closely related to the  $K$  to  $L$  x-ray coincidence measurements used to determine  $\omega_{KL}$ , the partial  $L$  shell yield following  $K$  x-ray emission. The fluorescence yield  $\omega_{KL}$  is a linear combination of  $\omega_{LII}$  and  $\omega_{LIII}$ , the fluorescence yields of the  $L_{II}$  and  $L_{III}$  subshells. The scintillation counters used to perform the coincidence experiments cannot separate the two components ( $K_{\alpha 1}$  and  $K_{\alpha 2}$ ) of the  $K_{\alpha}$  x rays, and thus the experiment determines only the average fluorescence yield  $\omega_{KL}$ . There are a number of elements possessing  $K$  absorption edges between the  $K_{\alpha 1}$  and  $K_{\alpha 2}$  x rays of the target materials. By using one of these elements as a secondary radiator, it is possible to eliminate all pulses in the  $K$  x-ray counter due to  $K_{\alpha 2}$  x rays. The only target x rays contributing to the coincidence rate are the  $K_{\alpha 1}$  x rays which are caused by  $L_{III} \rightarrow K$  transitions. The observed coincidence rate is therefore proportional to  $\omega_{LIII}$ . Values of  $\omega_{LII}$  can then be computed using previous measurements of  $\omega_{KL}$ .

### I. INTRODUCTION

THE first comprehensive measurements of  $L$ -shell fluorescence yields were made by using photoelectric absorption of certain characteristic x rays to create holes in the  $L$  shells of heavier atoms.<sup>1</sup> The fluorescence yields were then determined by measuring the intensity of the  $L$  x rays emitted after the ionization using photographic methods. Charged-particle bombardment has also been used to ionize the  $L$  shell, and proportional and Geiger counters have been employed to detect the resultant x rays.<sup>2</sup> Finally, a number of more recent experiments have been performed in which the vacancies in the  $L$  shell were created indirectly by the emission of  $K_{\alpha}$  x rays following  $K$ -shell ionization.<sup>3</sup> The average  $L$ -shell fluorescence yields measured by the methods outlined will, in general, be different from each other. The three subshells of the  $L$  shell,  $L_I(s_{1/2})$ ,  $L_{II}(p_{1/2})$ , and  $L_{III}(p_{3/2})$ , will be ionized in different ratios by the different methods described above. The approximate ionization ratio  $L_I:L_{II}:L_{III}$  for photoelectric absorption is 1:2:4; for electron bombardment it is 1:1:2; and for  $K_{\alpha}$  x-ray emission it is 0:1:2.<sup>4</sup> Since the fluorescence yields of the three subshells  $\omega_{L_I}$ ,  $\omega_{L_{II}}$ , and  $\omega_{L_{III}}$  are different, it follows that the average yields, which are linear combinations of the subshell yields, will also differ from each other. In principle, if three different linear combinations were measured experimentally, it would be possible to determine the fluorescence yield of each of the subshells. The difficulty with this procedure is that the actual ionization ratios of the subshells are not known with sufficient accuracy in any given experiment to make meaningful calculations possible.

The situation outlined in the previous paragraph is

\* Work done under the auspices of the U. S. Atomic Energy Commission.

<sup>1</sup> H. Lay, *Z. Physik* **91**, 533 (1935).

<sup>2</sup> H. Küstner and E. Arends, *Ann. Phys. (Leipzig)* **22**, 443 (1935).

<sup>3</sup> R. C. Jopson, H. Mark, C. D. Swift, and M. A. Williamson, *Phys. Rev.* **131**, 1165 (1963).

<sup>4</sup> A. H. Wapstra, C. J. Nijgh, and R. van Lieshout, *Nuclear Spectroscopy Tables* (North-Holland Publishing Company, Amsterdam, 1959).

somewhat improved if only the  $L_{II}$  and  $L_{III}$  subshells are considered. Reasonably good measurements of the average  $L$ -shell fluorescence yield following  $K_{\alpha}$  x-ray emission ( $\omega_{KL}$ ) exist.<sup>3</sup> This quantity can be expressed in terms of the subshell yields  $\omega_{L_{II}}$  and  $\omega_{L_{III}}$  as follows:

$$\omega_{KL} = I(K_{\alpha 2})\omega_{L_{II}} + I(K_{\alpha 1})\omega_{L_{III}}. \quad (1)$$

The coefficients are determined quite accurately by the relative intensities of the  $K_{\alpha 1}$  and  $K_{\alpha 2}$  emission lines for the element considered and are therefore well known (see Ref. 4). It now remains to devise a way of measuring another linear combination with coefficients which are equally well known in order to determine  $\omega_{L_{III}}$  and  $\omega_{L_{II}}$  separately.

### II. EXPERIMENTAL METHODS

The quantity  $\omega_{KL}$ , defined in Eq. (1), is determined by measuring the coincidence rate between  $K$  x rays and  $L$  x rays emitted after the  $K$  shell is ionized using a counter which cannot resolve the two  $K_{\alpha}$  x-ray components. This coincidence rate depends on  $\omega_{KL}$  and on the observed  $K$  x-ray counting rate in the following way:

$$N_e = N_K a(E_L A_L \Omega_L) \omega_{KL}, \quad (2)$$

where  $E_L$  is the efficiency of the  $L$  x-ray counter;  $A_L$  is the fraction of  $L$  x rays transmitted through the target, the air between the target, and the  $L$  x-ray counter and the  $L$  x-ray counter window; and  $\Omega_L$  is the geometrical factor of the  $L$  x-ray counter.  $N_K$  is the counting rate observed in the  $K$  x-ray counter and  $a$  is the fraction of  $K$  x-ray counts in the  $K$  x-ray counter caused by  $K_{\alpha}$  x rays.  $N_e$  is the coincidence counting rate. The essential point of the coincidence method is that the observation of a  $K_{\alpha}$  x ray (determined by the quantity  $aN_K$ ) indicates that a vacancy in the  $L$  shell has been created. The simultaneous observation of an  $L$  x ray thus determines the number of primary  $L$ -shell vacancies which are filled by radiative transitions. The fluorescence yield, which is the ratio of the number of vacancies filled by radiative transitions to the total number of vacancies created, is thus determined.

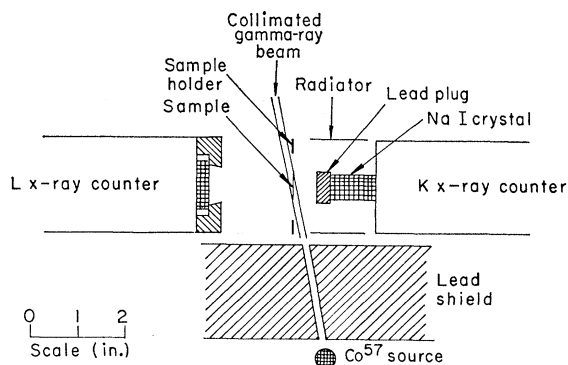


Fig. 1. The experimental arrangement used to measure  $\omega_{L_{III}}$ . The  $K$  x-ray counter is shielded from the direct  $K$  x-ray beam by the lead plug so that only  $K$  x rays produced in the radiator reach the crystal. The whole system shown above was placed in a controlled-temperature box not shown in this drawing.

The same coincidence method can be employed to measure the fluorescence yield of the  $L_{III}$  shell alone. This is accomplished by using a secondary radiator as shown in Fig. 1. The NaI scintillation crystal of the  $K$  x-ray counter is shielded from the direct  $K$  x rays produced in the target foil by a small lead plug. This must be done to insure that only  $K$  x rays produced in the secondary radiator are registered in the  $K$  x-ray counter. The  $K$  x rays produced in the target foil strike a cylindrical secondary radiator foil which surrounds the  $K$  x-ray counter. The  $K$  edge of the secondary radiator has an energy between the energies of the  $K_{\alpha_1}$  and  $K_{\alpha_2}$  x rays of the primary radiator, so that only the higher energy x ray ( $K_{\alpha_1}$ ) can produce  $K$  x rays in the secondary radiator. Two series of elements, one with  $Z=5$  (from  $Z=67$  to 73) and one with  $Z=6$  (from  $Z=78$  to 83) exist in the region of interest. (A list of element pairs in which this condition is met is shown in Table I.) A  $K$  x ray observed in the  $K$  x-ray counter thus must have been produced either by a  $K_{\alpha_1}$  or a  $K_{\beta}$  x ray originating in the primary radiator. No  $K_{\alpha_2}$  x ray can cause a signal in the  $K$  x-ray counter, and therefore no transitions  $L_{II} \rightarrow K$  in the target can contribute to the measured fluorescence yield. The fluorescence yield determined in this way is thus  $\omega_{L_{III}}$ . The coincidence rate is given by

$$N_c = N_K b (E_L A_L \Omega_L) \omega_{L_{III}}. \quad (3)$$

This equation is similar to Eq. (2), except that the factor  $a$  must be replaced by a new and somewhat more complicated function  $b$ . The factor  $a$  in Eq. (2) defines the fraction of the observed  $K$  x rays which result in  $L$ -shell vacancies. This is the ratio of the intensities of the  $K_{\alpha}$  x rays to the sum of all other  $K$ -series x rays, or

$$a = [N(K_{\alpha_1}) + N(K_{\alpha_2})] / \sum_i N(K_i). \quad (4)$$

In the present experiment, the  $K_{\alpha_2}$  x rays emitted by the target foil cannot cause  $K$  ionization in the radiator, so that the term  $N(K_{\alpha_2})$  must be omitted both in the numerator and the denominator of the fraction  $b$ . The

TABLE I. Elements between  $Z=67$  and 83 for which absorbers (radiators) exist having a  $K$  edge between the  $K_{\alpha_1}$  and  $K_{\alpha_2}$  x rays.

(Z-6) Series		(Z-5) Series	
Target	Radiator	Target	Radiator
Bismuth (83)	Iridium (77)	Tantalum (73)	Erbium (68)
Lead (82)	Osmium (76)	Hafnium (72)	Holmium (67)
Thallium (81)	Rhenium (75)	Lutetium (71)	Dysprosium (66)
Mercury (80)	Tungsten (74)	Ytterbium (70)	Terbium (65)
Gold (79)	Tantalum (73)	Erbium (68)	Europium (63)
Platinum (78)	Hafnium (72)	Holmium (67)	Samarium (62)

$K_{\alpha_1}$  and the other  $K$ -series x rays originating in the target foil can cause  $K$ -shell ionizations in the radiator; however, the absorption coefficients are somewhat different for each of the  $K$  x-ray lines, and this must also be accounted for in the calculation of  $b$ . Finally, the characteristic  $K$  x rays of the radiator are absorbed on the way out of the radiator. This effect must also be included in the computation of  $b$ . The following expression was used to obtain  $b$ :

$$b = C(K_{\alpha_1}) N(K_{\alpha_1}) / \sum_i C(K_i) N(K_i). \quad (5)$$

The factor  $C(K_i)$  accounts for the selective absorption of the incident and emergent x rays in the radiator. If the incident and emergent x rays are assumed to enter and leave the radiator at normal incidence, then  $C(K_i)$  is given by

$$C(K_i) = [\mu_K(K_i) / \mu(K_i) + \bar{\mu}_R] \times (1 - \exp\{-[\mu(K_i) + \bar{\mu}_K]t\}), \quad (6)$$

where  $\mu_K(K_i)$  and  $\mu(K_i)$  are the  $K$ -shell and total absorption coefficients of the  $K_i$  x ray, respectively,  $\bar{\mu}_R$  is the average absorption coefficient of the characteristic  $K$ -series x rays of the radiator in the radiator, and  $t$  is the thickness of the radiator. The sum in the denominator of Eq. (5) includes only the  $K_{\alpha_1}$ ,  $K_{\beta_1}$ , and  $K_{\beta_2}$  x rays, since the other lines are sufficiently weak so that they can be ignored without substantially changing the value of  $b$ . The dependence of  $b$  on the angles of the incoming and outgoing x rays was determined by properly modifying Eq. (6) and performing calculations assuming a number of different incident and emergent angles between normal incidence and  $45^\circ$ . In no case did the value of  $b$  differ by more than 3% from the value computed assuming normal incidence. Use of Eq. (5) to calculate  $b$  is therefore appropriate.

The value of  $N_K$ , which is the true  $K$  x-ray counting rate in the  $K$  counter, is obtained from the observed counting rate by subtracting appropriately measured background counting rates. The background due to Compton scattering and Rayleigh scattering of the  $\text{Co}^{57}$  gamma rays in the target foil was measured by placing a 10.8-mg/cm<sup>2</sup> copper foil in the gamma-ray beam. Rayleigh scattering in the radiator was measured by using a target foil made of the same material as the radiator. In this case, no  $K$  x rays produced in the target foil can produce  $K$  ionization events in the radiator. All

TABLE II.  $L_{II}$  and  $L_{III}$  shell fluorescence yields.

Element	Z	Present results	$\omega_{LIII}$			Others	$\omega_{LII}$			
			Kinsey <sup>a</sup>	Küstner and Arends <sup>b</sup>	Roos <sup>b</sup>		Kinsey <sup>a</sup>	Küstner and Arends <sup>b</sup>	Roos <sup>b</sup>	Others
Bismuth	83	0.37±0.05	0.30	0.367			0.51±0.08	0.46	0.255	
Lead	82	0.35±0.05		0.337	0.35 ±0.04		0.50±0.08		0.264	0.24±0.04
Thallium	81	0.37±0.06	0.27			0.33 <sup>e</sup>	0.57±0.10	0.43		
Mercury	80	0.32±0.05				0.34 <sup>d</sup>	0.58±0.10			0.42 <sup>d</sup>
Gold	79	0.31±0.04	0.25	0.276	0.32 ±0.03		0.50±0.08	0.39	0.272	0.27±0.04
Platinum	78	0.31±0.04		0.262	0.275±0.03		0.46±0.07		0.274	0.31±0.04
Tantalum	73	0.25±0.03	0.18	0.191	0.23 ±0.02		0.37±0.06	0.31	0.326	0.23±0.04
Hafnium	72	0.22±0.03					0.37±0.06			
Lutetium	71	0.22±0.03					0.33±0.06			
Ytterbium	70	0.20±0.02					0.34±0.05			
Erbium	68	0.21±0.03					0.21±0.04			
Holmium	67	0.22±0.03					0.22±0.04			

<sup>a</sup> See Ref. 6.  
<sup>b</sup> See Refs. 2, 5.  
<sup>c</sup> H. Winkelnbach, Z. Physik **152**, 387 (1958).  
<sup>d</sup> S. K. Haynes and W. T. Achor, J. Phys. Radium **16**, 635 (1955).

the counts appearing in the  $K$  x-ray window of the counter must therefore come from elastic (i.e., Rayleigh scattering) of  $K$  x rays from the target foil by the radiator. Finally, background counts due to cosmic rays and multiple-scattered source gamma rays were determined by measuring the counting rates with no foil in the target position.

Equation (3) shows that it is necessary to know the solid angle subtended by the  $L$  x-ray counter. If the distance between the target foil and the counter is large (~4 in.) then the inverse square law is valid for computing the geometry. At smaller distances, the geometry was determined by measuring the effective source strength of a target foil (using copper  $K$  x rays) at a large foil-to-counter distance and then using the foil as a calibrated source to measure the geometry at smaller distances. Each  $\omega_{LIII}$  measurement was made at two different counter-to-target distances. The results obtained using different geometries differ from each other by an average of 3-5%, showing that the method of measuring  $\Omega_L$  is self-consistent. The final values of  $\omega_{LIII}$  were obtained by averaging the results of the measurements made with two different target-to-counter distances.

Standard electronic equipment was used for the coincidence measurements. The  $L$  x-ray counter was a cleaved-crystal NaI(Tl) scintillation counter similar to the one described in Ref. 3. The counting rates were quite low: of the order of one coincidence count every 1 to 10 min. The  $K$  and  $L$  x-ray counting rates in the respective windows were of the order of 100 to 1000 counts/min. The relatively low coincidence rates made it necessary to operate the equipment for long periods. The whole system was therefore placed inside a temperature-controlled box to stabilize the phototube gains.

III. DISCUSSION OF RESULTS

Twelve measurements of  $\omega_{LIII}$  were made and results given in Ref. 3 were used to compute  $\omega_{LII}$  from  $\omega_{KL}$ .

These are shown in Table II together with some previous measurements of  $\omega_{LIII}$  and  $\omega_{LII}$ . The present measurements of  $\omega_{LIII}$  are in reasonably good agreement with the old measurements of Küstner and Arends<sup>2</sup> and also the more recent numbers obtained by Roos.<sup>5</sup> As in the case of the previous measurements of  $\omega_{KL}$ ,<sup>3</sup> the present numbers given for  $\omega_{LIII}$  are somewhat larger than those obtained by Kinsey<sup>6</sup> from the comparison of emission line and absorption edge widths. In the case of  $\omega_{LII}$ , the situation is different. Kinsey's values are again too low,

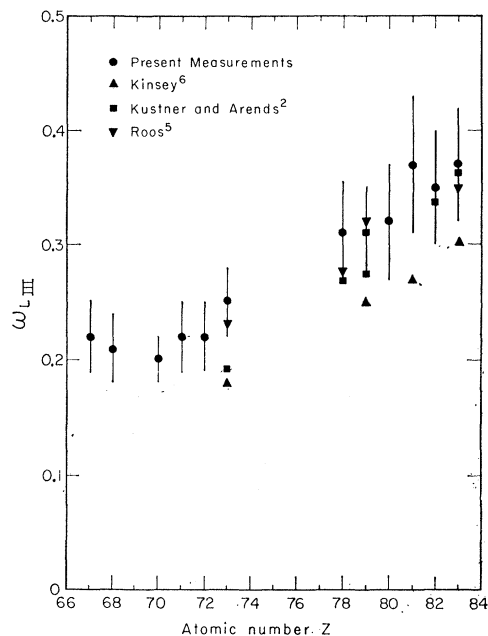


FIG. 2. The measured values of  $\omega_{LIII}$ . The results of some previous measurements are also shown.

<sup>5</sup> C. E. Roos quoted in B. L. Robinson and R. W. Fink, Rev. Mod. Phys. **32**, 117 (1960).  
<sup>6</sup> B. B. Kinsey, Can. J. Res. **A26**, 404, (1948).

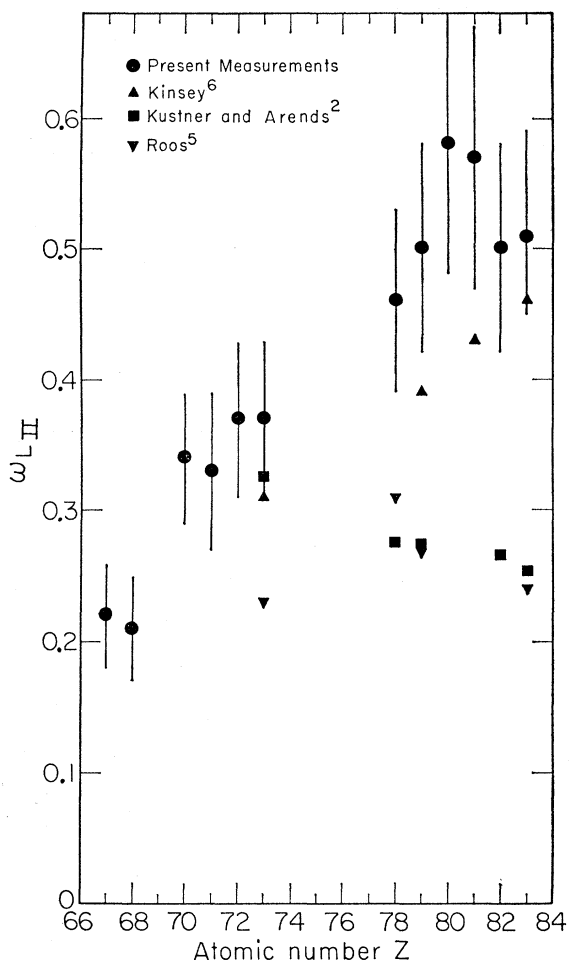


FIG. 3. The measured values of  $\omega_{LII}$ . The results of some previous measurements are also shown.

but they show the same trend as the present results in that they increase as  $Z$  increases. The results obtained by Roos and by Küstner and Arends show the opposite behavior. Also, the numbers themselves are not in good accord with the present measurements. Figures 2 and 3 show the results compared to some previous measurements.

The errors quoted for the measurements of  $\omega_{LIII}$  are quite large. The standard error in the values of  $\omega_{LIII}$  is between 10 and 17%, depending on the type of target used. As in the case of the measurement of  $\omega_{KL}$ , the un-

certainty in measuring the thickness, and hence estimating the self-absorption of the oxide target, introduces a larger error than in the case of the pure-metal targets. The statistical deviations were held to  $\pm 3\%$  by accumulating at least 1000 coincidence counts. For thin targets (i.e., low counting rates) it often took at least a week to do the experiment. The measured background count rates in the  $K$  x-ray counter were quite high, between 20 and 50%, and the coincidence background plus random rates were roughly 10%. These background effects, as well as uncertainties in estimating the geometrical and absorption factors in Eq. (3) contribute to the relatively large standard errors quoted in Table II. The standard errors quoted for the values of  $\omega_{LII}$  are larger than those given for  $\omega_{LIII}$  since the standard deviations in  $\omega_{KL}$  must be included. As in Ref. 3, larger errors are quoted for those cases where oxide targets must be used.

Finally, some comments should be made regarding the behavior of  $\omega_{LII}$  and  $\omega_{LIII}$ . For the low values of  $Z$  (holmium and erbium)  $\omega_{LII}$  and  $\omega_{LIII}$  are equal within the uncertainty of the present measurements, whereas for the large values of  $Z$ ,  $\omega_{LII}$  is substantially larger than  $\omega_{LIII}$ . Also, both  $\omega_{LII}$  and  $\omega_{LIII}$  increase as  $Z$  increases. Both of these observations are in accord with expectations; however, no really good quantitative theoretical calculations exist with which the present results can be compared. Qualitatively, radiative transitions become more probable compared to nonradiative ones as the energy of the transition increases. Thus, both  $\omega_{LII}$  and  $\omega_{LIII}$  should increase as  $Z$  increases. A similar argument can be applied to explain the behavior of the relative values of  $\omega_{LIII}$  and  $\omega_{LII}$ . As  $Z$  decreases, the relative difference in the binding energy of the  $LII$  and  $LIII$  shells decreases. (That is, the ratio of the binding energies approaches unity.) Thus, it follows that the fluorescence yields of the two subshells should become equal as  $Z$  becomes smaller. In all these arguments the effects of Coster-Kronig transitions have been ignored. This procedure is legitimate for the values of  $Z$  considered here since there are no prominent Coster-Kronig transitions between the  $LII$  and  $LIII$  shell in this region.

#### ACKNOWLEDGMENTS

The authors would like to express their thanks to Arnold Kirkewoog and Edward Zaharis for their help during the course of this work.